https://doi.org/10.1002/jsfa.13435

Title

Feasibility of excitation-emission fluorescence spectroscopy in tandem with chemometrics for quantitation of *trans*-resveratrol in vine shoots ethanolic extracts

Running title

Analysis of resveratrol by fluorescence and multiway methods

Authors

Antonio F. Caputi[1], Giacomo Squeo[1*], Ewa Sikorska[2], Roccangelo Silletti[1], Mirella Noviello[1], Antonella Pasqualone[1], Carmine Summo[1], Francesco Caponio[1]

1 Department of Soil Plant and Food Sciences (Di.S.S.P.A.), University of Bari Aldo Moro, Via Amendola 165/A, 70126 Bari, Italy

2 Institute of Quality Science, Poznań University of Economics and Business, al. Niepodległości 10, 61875 Poznań, Poland

* Corresponding author: giacomo.squeo@uniba.it

Abstract

Background. *Trans*-resveratrol (TR) is a well-known phytochemical compound with important biological properties, that could be recovered from agri-food by-products or wastes, such as vine shoots. Once recovered, its concentration should be measured, possibly in a green, non-destructive, and efficient manner. With these premises, this work aims to explore the feasibility of excitation-emission fluorescence spectroscopy combined with chemometrics for the analysis of TR in raw extracts obtained from vine shoots. A total of 75 extracts were produced and analysed by UPLC-DAD and spectrofluorimetry. Then, the feasibility of two calibration strategies (a PARAFAC based calibration and the NPLS regression) for TR quantitation was assessed.

Results. The extracts showed a variable content of TR, whose excitation/emission maxima were at around 305/390 nm, respectively. The best PARAFAC based calibration allows to obtain a RMSEP = 22.57 mg L^{-1}, and an RPD = 2.91 but a large number of PARAFAC components should be considered to improve the predictions. The results of the NPLS regression were slightly better, with a RMSEP = 19.47 mg L^{-1}, and an RPD = 3.33, in the best case.

Conclusion. Fluorescence could be an alternative analytical technique to measure TR in complex samples. Chemometrics tools allowed the identification of the TR signal in the fluorescence landscapes that could be further used for its non-destructive quantitation. The needing of a more accurate criterion for the optimal PARAFAC complexity emerged.

Keywords: Stilbenes; by-products; chemometrics; multiway; PARAFAC; NPLS.

Introduction

Stilbenoids are a family of natural polyphenolic compounds deriving from the secondary metabolism of many plants, known as phytoalexins. Their synthesis occurs primarily to cope with plant biotic stresses.[1] However, abiotic factors have also been shown to contribute to their formation (e.g., to protect plants from UV damage).[2,3] In recent years, numerous studies have been carried out on this category of compounds, especially on *trans*-resveratrol (TR), which is considered one of the most scientifically interesting stilbenes. Researches have shown that TR possesses important antioxidant, antimicrobial, antiaging, and anti-inflammatory properties; it has neuroprotective and cardioprotective functions; and it acts as an inhibitor of cell proliferation.[4-7] According to some authors, this stilbene could be used as an alternative anti-phytopathogen to protect plants such as grapevines from the most notorious fungal attacks and as a preservative to be used in post-harvest to protect fruits and vegetables. [8,9]

Since TR shows important benefits for health, agriculture, and other applications, its demand is expected to increase in multiple sectors.[10] In this context, attention is being turned to convenient sources of this compound, such as agri-food by-products and wastes. It is known that *Vitis vinifera* L. constitutes an excellent source of TR, which is found distributed throughout the whole plant, with relevance in the vine shoots, one of the main wastes of the grape/wine supply chain.[11] According to the literature, the concentration of TR in the vine shoots is mainly related to factors such as variety, geographical area, climatic conditions, and practices such as the storage of the vine shoots after pruning.[10-14] Recently Noviello et al. (2022)[15], have proven that the heat pre-treatments applied to vine shoots before the extraction process had a slight impact on the TR concentration, compared to the genotype, which was the most important variable. Finally, also the extraction method has a crucial effect on the recovery of TR. Several works have investigated the use of solid-liquid extraction methods, even

combined with emerging technologies (such as ultrasound-assisted extraction or microwave-assisted extraction), to obtain raw TR-rich extracts from vine shoots. [14-15]

Apart from TR recovery, the need to develop analytical methods for its measurement has been highlighted. [16]

Typically, the quantification of TR is carried out by high-performance liquid chromatography (HPLC) coupled with diode array detection (DAD) or mass spectrometry (MS).[11,16] These traditional approaches allow targeted detection of TR, but have some limitations, as they are expensive and time-consuming. Moreover, due to the huge consumption of organic solvents they cannot be considered "green", and their applicability out of the labs or for real-time monitoring are challenging. Basically, chromatography has the advantage of allowing the separation of TR from other analytes in the complex mixtures in which it could be found, and to quantify it by means of a proper calibration strategy. However, it is interesting to know that the term "stilbene" derived from the Greek word "stilbos" meaning "shining", that could be associated to the ability of stilbenes to emit light when excited by UV radiation.[11] Hence, by leveraging the fluorescent properties of TR, and through the application of suitable chemometric tools [17] to the fluorescence signal of TR containing samples, chromatographic-like benefits, such as signal extraction and quantification, could be obtained. In this case, the use of solvents and time is significantly reduced while the selectivity and sensitivity, typical of fluorescence spectroscopy are retained.[18] Furthermore, fluorescence spectroscopy is already successfully used as non-destructive technique for on-line measurement in different fields.[19]

Several types of fluorescence spectroscopy exist, but, in the case of multicomponent systems, the most comprehensive characterization of a sample is obtained by collecting the excitation-emission matrix (EEM).[18] A EEM consist of a series of emission spectra recorded at different excitation wavelength and represents a unique fingerprint of the measured sample. Each EEM of a sample is a data matrix

(excitation λ × emission λ) whose entries are the fluorescence intensity values per each excitation-emission combination. When more EEMs are collected, these could be stacked one over the other, resulting in a 3D data cube (also called a three-way array), and properly treated by using multiway chemometric methods.[17,18,20] Among these, parallel factor analysis (PARAFAC), N-way partial least squares (NPLS), are the most widely used algorithms for the exploration, characterization and quantification of fluorescent compounds present in food and non-food matrices.[20]

Based on these considerations, the present study aimed at assessing the feasibility of excitation-emission fluorescence spectroscopy combined with chemometrics for the analysis of TR in a complex matrix, represented by the raw ethanolic extracts obtained from vine shoots of several *Vitis vinifera* L. varieties.

Materials and methods

Chemicals and Reagents

Methanol (≥99.9%) was purchased from Honeywell (Honeywell International, Inc., Morristown, NJ, USA) while glacial acetic acid (≥99.7%) from JT Baker (Avantor Performance Materials LL, Center Valley, PA). All solvents were HPLC grade. Ultrapure water from an Elga Purelab Option R system (Veolia Environnement S.A., Paris, France) was used for preparing all solutions. Finally, ethanol for analysis (≥99.8%) was obtained from VWR (VWR BDH Chemicals, Rou d'Aurion, France) while *trans*-resveratrol standard from United States Pharmacopeia (USP, Rockville, MD, USA).

Plant materials

Vine shoots were collected in two different periods. The first set (dataset A, n = 52) include vine shoots collected in winter 2021 from a varietal collection located in Locorotondo (Puglia, Italy; coordinates: longitude 17°13'3.741" E, latitude 40°45'42.763" N), representative of 23 different varieties of *Vitis vinifera* L, together with vine shoots subjected to different post-harvest treatments, as reported in

Noviello et al.[15] The second series of samples (dataset B, n = 23) was collected in spring 2022 in part from the same collection located in Locorotondo (as dataset A), and partly from a vineyard located in Laterza (Puglia, Italy; coordinates: longitude 16°78'3.448" E, latitude 40°71' 1.255" N). These samples were representative of other 13 different varieties of *Vitis vinifera* L. For those varieties of which large amounts of vine shoots were available, at least two different specimens were collected and analyzed independently to extend the covered range of TR concentrations.

Extracts production and chromatographic analysis of TR

The raw extracts were obtained as reported by Noviello et al.[15] In brief, after air drying, vine shoots were manually cut with a pruning shear (size about 2 cm long), milled using a hammer mill (Dietz-Motoren KG, Elektromotorenfabrik, 7319 Dettingen-teck, Germany), and immediately subjected to TR extraction performed according to Vergara et al.[21] with some modifications. About 2 g of ground vine shoots was added with 16 mL of an ethanol/water solution (80:20 v/v) and sonicated in an ultrasonic bath (CP104 Standard Ultrasonic Cleaning Machine, CEIA, Padova, Italy) at room temperature and 50 Hz for 5 min. The extract was centrifuged at 10 000 × *g* for 5 min (SL 16R Centrifuge, Thermo Fisher Scientific, MA, USA), the supernatant was separated, filtered through Whatman filter paper (GE Healthcare, Milan, Italy) (67 g m^{-2}), and then filtered using 0.45 µm nylon filters (Sartorius Stedim Biotech Gmbh, Göttingen, Germany). The extraction was carried out once per sample. Once produced, the extracts have been stored at -18 °C and, before analysis, thawed and balanced at room temperature.

Raw vine shoots extracts were analyzed by UHPLC-DAD as described in Noviello et al.[15] Specifically, a UHPLC Dionex Ultimate 3000 system (Thermo Scientific, Munich, Germany) was used, consisting of an HPG-3200RS binary pump, WPS-3000RS autosampler, TCC-3000RS column oven, a DAD-3000RS photodiode array detector, and a fluorescence detector FLD-3400RS. HPLC separation was achieved by an Acclaim™ C18 column (120 Å 3 × 150 mm, 3 µm) maintained at 25 °C, using a mobile phase consisting

of 1% (v/v) acetic acid in Milli-Q water (A) and methanol (B). The flow rate was 0.6 mL min^{-1} under the following gradient elution conditions: 0 min (20% B), 10 min (20% B) 6.5 min (37% B), 12.6 min (50% B) and 21.0 min (100% B). Under these conditions, TR retention time was 14.5 ± 0.1 min. The chromatograms were recorded at 306 nm. Quantification of TR was achieved by an external calibration curve prepared using TR standard solutions in the concentration range of 1-500 mg L^{-1} (R^2 = 0.9993). The chromatograms were also registered by the FLD detector, set at an excitation wavelength of 350 nm and at an emission of 380 nm. The mean TR value of two technical replicates was reported and used for the multivariate data analysis.

Standard solutions of TR for PARAFAC based calibration

Four standard (STD) solutions of TR (20, 50, 100, and 200 mg L^{-1}) in ethanol/water (80/20, v/v) were prepared for the development of a PARAFAC based calibration model and submitted to fluorescence analysis. The excitation (at emission = 380 nm) and emission (at excitation = 300 nm) spectra of the TR standard solution at 200 mg L^{-1} were used as references for comparison with the excitation and emission loadings profiles of the factors extracted by PARAFAC. The EEMs were collected once per each STD solution.

Spectrofluorimetric analysis

The fluorescence measurements were carried out by using a Fluoromax 4 spectrofluorometer (Horiba Scientific, New Jersey, USA), in a right-angle acquisition geometry. Before each measurement, the extracts or the STD solutions were diluted 1:100 with the extraction mixture (ethanol/water, 80/20 v/v). EEMs were obtained by recording the emission spectra from 275 to 500 nm, with excitation wavelengths ranging from 220 to 360 nm, at 5 nm steps. The excitation and emission slits were set to 2 nm. The integration time was 1 s. The measurements were made in quartz cuvettes with an optical path length of 1 cm. A EEM of the blank (ethanol/water, 80/20 v/v) was collected under the same conditions. During

each measurement, the raw signal (S), the corrected signal (Sc), and the corrected reference signal (Rc) were acquired. The final signal used for further processing was the corrected and normalized signal (Sc/Rc). The EEMs were collected once per each sample. The pH of 20 diluted samples was measured by a pHmeter (Hanna edge® HI2020, Hanna Instruments, Villafranca Padovana, Italy).

Data elaboration and statistical analysis

All the multiway data elaboration were carried out in MATLAB environment (R2021a, The MathWorks, Inc., Natick, MA, USA), using built-in functions and the PLS_toolbox 9.1 (Eigenvector Research Inc., Manson, WA, USA). The EEMs were exported as excel files (Microsoft, Redmond, WA, USA), imported in MATLAB, and arranged in a three-way array (sample × excitation λ × emission λ). The array was then preprocessed by blank subtraction and first order Rayleigh scatter removal (half-width 5 nm) followed by replacement with interpolated data. Two different regression approaches were followed.

The first one was a PARAFAC based calibration model as reported in [22]. Each EEM is matrix of size J × K, where J is the number of excitation λ, and K is the number of emission λ. When more than one sample are present, these EEMs can be organized into a three-dimensional array, or a 3D data cube, with dimensions equal to I × J × K, where I represents the number of samples. Each entry in this array contains a value, identified by the three indices (*i*, *j*, *k*), representing the fluorescence intensity of the *i*th sample for the *j*th emission λ and the *k*th excitation λ. PARAFAC allows to decompose this three-dimensional array into a set of trilinear components (or factors) that, under ideal conditions, suitable constrains, and a proper choice of the number of components, correspond to the fluorophores in the samples. In other words, PARAFAC extracts, or resolve, chemical meaningful signals from complex and multicomponent fluorescence landscapes. Being a trilinear decomposition, each component is described by a set of three loadings that correspond to i) the emission profile of the fluorophore, ii) the excitation profile, and iii)

the corresponding relative abondance within the samples of the dataset. In mathematical terms we have the following equation:

$$x_{ijk} = \sum_{f=1}^{F} a_{if} \times b_{jf} \times c_{kf} + e_{ijk} \quad [23]$$

where x_{ijk} is the fluorescence intensity registered for sample *i*, at the excitation wavelength *j*, and at the emission wavelength *k*. The trilinear array is decomposed into a triad made of sample loadings a_{if}, excitation loadings b_{jf}, and emission loadings c_{kf} for each component f. Variations in the data not captured by the model are represented by the residual term e_{ijk}. For more details about PARAFAC the reader is referred to other sources. [22-24]

Hence, following the first regression strategy [22], a unique tensor was built including the EEMs of the TR STD solutions together with those of the samples (79 × 29 × 46). Then, it was decomposed by PARAFAC and, once the component of interest has been identified (in our case the one associated with TR) a linear calibration model was developed in the form: sample mode loadings *vs* TR concentration (of the STD solutions). Then, with this calibration line, the TR concentration in the extracts has been calculated (i.e., the predicted concentrations) starting from the PARAFAC loadings in the sample mode, and the predicted *vs* measured concentrations of TR have been compared. A schematic representation of this regression approach is reported in Figure S1. For PARAFAC decomposition, the non-negativity constraint was set for all the modes and core-consistency (CONCORDIA), split-half analysis, total variance explained, model residuals, loadings' meaningfulness, and loadings' correlation with the excitation and emission spectra of the TR standard were the diagnostics used to define the proper number of PARAFAC components.

The same elaboration was done also considering a reduced emission range, excluding the emissions wavelengths below 335 nm, as further discussed in the Results and Discussion section.

192 The second regression approach was NPLS. In this case, in the begin the whole dataset (n = 75) was split
193 into a calibration set (n = 50) and a validation set (n = 25) by the onion algorithm of the PLS_toolbox.
194 The calibration set was preprocessed as already reported for PARAFAC, plus the mean-centering over
195 the sample mode. The optimal number of latent variables (LVs) was defined by minimizing the cross-
196 validation error (7 random splits and 5 iterations). Two NPLS regression models were developed using
197 the full and the reduced emission range. The regression models were assessed by the coefficient of
198 determination (R^2), the root mean square errors (RMSE) in calibration (C), cross-validation (CV), and
199 prediction (P), the percentage relative error in prediction (RE) and the relative prediction deviation
200 (RPD) [25].
201
202 **Results and discussion**
203 *Trans-resveratrol content of vine shoots extracts by reference analysis*
204 Table 1 shows the concentration of TR in the analyzed vine shoots extracts.
205 **Table 1.**
206 The mean concentration of TR was 93.03 mg L^{-1} but varied strongly depending on the variety and the
207 dataset considered. Minimum and maximum values of 0.42 and 203.90 mg L^{-1} were registered for
208 Malvasia Bianca and Negramaro, respectively, with an overall range equal to 203.48 mg L^{-1}. Numerous
209 studies have shown that variety is an important factor influencing the content of phenols in grapes and
210 vines.[15,21,26] Many authors have found an important difference between white and red varieties, with
211 the latter having the highest content of polyphenols.[27,28] Moreover, other factors such as the
212 geographical location of the vineyard, the climatic conditions, the environmental stresses (such as sun
213 exposure, temperature and the amount of water available), and even the mechanical treatments
214 applied to the vine shoots (such as pruning, post-pruning conservation), affect the phenols content.

215 Finally, the concentration that could be found in raw extracts is also dependent on the kind of extraction
216 used.[14] Overall, to our aim of developing and testing regression models for TR quantitation based on
217 fluorescence, the great variability observed is welcome, allowing to cover a wide range of
218 concentrations.

219 *Fluorescence characteristics of vine shoots extracts*

220 Figure 1 depicts the fluorescence landscape of four different specimens, two from dataset A (No. 48 and
221 31 in Table 1) and two from dataset B (No. 68 and 67 in Table 1), having low and high TR concentration,
222 respectively.

223 **Figure 1.**

224 As it could be observed, the fluorescence landscape could be different among the samples although the
225 overall shape is quite consistent.

226 Two main fluorescence emission bands could be distinguished, characterized by excitation/emission
227 maxima at nearly 235, 275/310 nm, and 240, 305/390 nm, respectively. In the samples with low TR
228 concentration (Figure 1A and Figure 1C) emerged also an emission band at 390 nm with excitation at
229 260 nm, that is probably masked when the intensity of the TR signal is predominant. According to the
230 literature data, these bands could be associates with phenolic compounds, amino acids, or vitamins.[29]
231 TR was reported to have excitation/emission maxima at 300/360 nm[30], 330/400 nm[20], or 300/380 nm[31],
232 depending on the solution considered and, consequently, it could be associated with our observed
233 emission band at around 400 nm (Figure 1). It should be considered that environmental factors can
234 cause shifts in the fluorescence peaks[32] and, in the case of TR, the pH affects its acid–base equilibria and
235 isomerization, modifying the observed maxima.[31] However, in our case, the pH among the samples was
236 quite similar (5.15 ± 0.12, n = 20) (indeed all were diluted 1:100 with the ethanol/water (80/20 v/v)

237 mixture before the fluorescent measurements) and the observed TR fluorescence profiles were
238 comparable to those reported in this weak acidic condition.[31]
239 The EEMs of other samples (data not shown) were consistent with the one presented in Figure 1 for
240 what concern the bands position (i.e., the excitation/emission maxima), although the fluorescence
241 intensity pattern varied. In general terms, the observation of the fluorescence landscapes let us assume
242 that i) the extracts were characterized by almost similar fluorophores, ii) whose amount (absolute and
243 relative) in the extracts was different. For what concern the first assumption, the UHPLC-FLD data (Figure
244 2) suggested the presence of 4 to 6 major fluorescent species, plus an unspecified number of other
245 minor contributors (considering the detector excitation/emission settings). The second assumption is
246 corroborated, for what concern TR, by the reference data which proved the great variability of such
247 stilbene in the extracts under study (Table 1).
248 **Figure 2.**
249 *Regression models for TR quantitation*
250 The fluorescence landscapes prove that a signal referable to TR was present allowing us to proceed with
251 the development of regression models for TR quantitation. For three-way data different regression
252 approaches could be used, such as i) the bilinear PLS on the unfolded three-way array, ii) PARAFAC based
253 calibrations, iii) the *N*PLS.[24,33] The application of common PLS has the disadvantage of requiring a
254 bilinear decomposition of trilinear data. Thus, in this work this strategy was not followed, although other
255 reports showed good results.[34,35] On the other hand, PARAFAC based calibrations have shown good
256 results[22] and are often preferred because offer the so-called second-order advantage, i.e., the
257 mathematical separation of the analyte signal and its determination in the presence of unmodeled
258 components/interferents that are not included in the calibration set.[36,37] Thus, as a first approach, we
259 tested the feasibility of a PARAFAC based calibration. The first step has been the decomposition of the

augmented tensor (79 × 29 × 46) to retrieve the signal ascribable to TR to be used in the regression. Table 2 reports the results of the PARAFAC decomposition.

Table 2.

The results showed that by increasing the model complexity, the CONCORDIA value tend to decrease, as already known [24], as well as the split-half quality. On the other hand, the explained variance of the PARAFAC model tend to increase, more consistently up to the 5th component and, after that, only slight improvements are registered up to the 12th component. The average model residuals (Figure S2) are in accordance with these observations. Considering the profiles of the extracted factors (Figure 3 and Figure S3), the 1-component model was clearly under-specified, with both the excitation and emission profiles not-well resolved. Thereafter, more meaningful profiles were progressively extracted and, at the same time, an increasing correlation of one of the extracted components with the excitation and emission profiles of TR STD was observed (Table 2).

Figure 3.

At a first glance, the optimal model complexity, that allowed to extract the factor that best correlates with TR excitation and emission spectra, seem to have 5 or 6 components. In both the cases, component 1 was the best correlated, and thus ascribable, to TR. Following, a calibration line was built by using the PARAFAC loadings in the sample mode of the STD solutions (considering component 1; Figure 3) and the relative concentrations and used to predict the TR concentrations in the extracts. The results are presented in Table 3, while Figure 4 shows the fit and predicted *vs* measured concentrations plot for the 6-components PARAFAC model.

Table 3.

Figure 4.

The regression models in calibration were excellent, as shown by the R^2 and the RMSEC. However, when it comes to predict the TR concentration in the extracts, a general over-estimation of TR was observed (Figure 4B). The results were poor and unsatisfactory with a very high RMSEP and relative error. The RPD values could also be considered as very poor.[38] These bad results in prediction might be due to a non-optimal extraction of the TR component by the PARAFAC model. In fact, if the signal is not well resolved, suffering from the overlapping of other fluorophores, additive effects could cause an over-estimation. With this regard, Halberg and colleagues[39] have critically shown that in real complex matrices, as it could be considered an ethanolic extract from vine shoots, often more components than those found optimal by common metrics (such as core consistency or split-half analysis) should be considered. In our study, this observation is corroborated by Figure 2 that shows that a higher number of minor fluorophores could be observed by HPLC.

According to these premises, the best results were obtained with a 12-components model. Figure 5 shows the fit and predicted *vs* measured concentrations plot while in Table S2 the predicted TR concentrations could be observed.

Figure 5.

In this case, by using the factor ascribed to TR (factor no. 2), the improvement in the prediction performance respect to the 5 or 6 component model is evident (Table 3). Thus, although some of the extracted components' loadings could not have a clear chemical meaning, it seems worthing extracting them in order to retrieve a better resolved TR component.

Considering that the lower emission wavelengths were dominated by other signals, not ascribable to TR (Figure 1), we also tried to reduce the emission range deleting the emission < 335 nm. With this new dataset (79 × 29 × 34) the same strategy presented for the full emission range was followed. Even in this case, with a few number of components the predicted concentrations were over-estimated. By

increasing the number of PARAFAC components, it was observed an improvement of the results, again up to 12 components. The prediction results were little worse (R^2 = 0.876, a RMSEP = 22.99 mg L^{-1}, a RE = 25%, and an RPD = 2.85) than those obtained by using the full emission range.

As already commented, it seems that many components should be considered to reduce the prediction error and, overall, it emerged that the optimal PARAFAC complexity for the subsequent quantitation of TR could not be easily achieved by only considering the best correlation with the TR excitation/emission spectra. The need of a more accurate criterion came up. On the other hand, the second order advantage of PARAFAC based calibration emerged, as it has been possible to predict the TR content in complex samples having several interferent signals by only calibrating the system on four TR standard solutions. Despite the prediction of TR in our context has been revealed challenging, the results appear promising and in line, or even better, than those reported by Cabrera-Bañegil et al. (2019)[20] for the prediction of TR in diethyl ether extracts of grapes, although the regression strategy was not the same. In fact, the authors reported a relative error of prediction (REP) of 20.01% in calibration while, in prediction, the REP increased reaching 56.62%. At the same time, it is worth recall that the use of PARAFAC based calibration has demonstrated effectiveness in different contexts. Examples span from the agri-food sector, to the clinical one, and others.[22-24]

Finally, also NPLS regression models were computed. Table 4 reports the results of the regression, while Table S1 presents the statistics of the calibration and validation sets. The established regression models were satisfactory in both calibration and cross-validation. Furthermore, a good prediction accuracy was obtained. The performance of the models was almost similar considering the entire or the reduced emission range, although the former performed slightly better, in accordance with what already observed in the case of PARAFAC based calibration. The predictions of the TR concentration in the test set could be observed in Table S2.

328 **Table 4.**

329

Conclusions

The development of rapid methods for quantitation of bioactive compounds is a hot topic that matches the modern requirement of clean analytical methods, and chemometrics tools offer an unvaluable help to reach this goal. *Trans*-resveratrol is an important bioactive found in food but also used as supplement in diets or in the cosmetics field and its recovery from wastes or by-products is welcome. It has been proved that ethanolic extracts of vine shoots could be a source of TR which, in any case, should be quantified. Given his fluorescence properties, the feasibility of a spectrofluorimetric method coupled with chemometric has been tested. The results showed that raw vine shoots extracts are variable in TR concentration as well as for what concern the presence and abundance of interfering compounds. PARAFAC decomposition allow to retrieve a component with excitation and emission profiles highly correlated with those of standard TR, suitable for its quantitation. Nonetheless, based solely on this criterion, the optimal components model gave a biased estimation of TR that could be linked to interference from other fluorescent components.

The prediction was improved by increasing the number of PARAFAC components used in the tensor decomposition. The second-order advantage seems thus exploited, although the need of an objective way of selecting the best number of PARAFAC factors emerged, as the sole correlation of a factor with TR excitation and emission spectra did not ensure the optimal results. The NPLS regression gave also promising results, slightly better than those observed with the PARAFAC based calibration.

Overall, considering the general aim of this work, we can conclude that fluorescence spectroscopy in tandem with chemometrics seems promising for the development of non-destructive, convenient, and rapid methods of analysis of TR in complex matrices, although more efforts are needed to rich a definitive analytical protocol. This could open the doors to new and innovative applications in the agri-food sector, also matching the latest trends in on-line and real-time measurements.

Conflict of interest

All authors have declared no conflicts of interest.

Credit author statement

Antonio Francesco Caputi: Conceptualization, Formal analysis, Investigation, Writing - Original Draft, Writing - Review & Editing; Giacomo Squeo: Conceptualization, Methodology, Software, Formal analysis, Investigation, Writing - Original Draft, Writing - Review & Editing; Ewa Sikorska: Conceptualization, Methodology, Formal analysis, Writing - Review & Editing; Roccangelo Silletti: Investigation, Writing - Review and Editing; Mirella Noviello: Investigation, Formal analysis, Writing - Review & Editing; Antonella Pasqualone: Visualization, Writing - Review & Editing; Carmine Summo: Formal analysis, Writing - Review & Editing; Francesco Caponio: Conceptualization, Resources, Writing - Review & Editing, Supervision, Project administration. All authors have read and agreed to the published version of the manuscript.

References

1. Jeandet P, Douillet-Breuil AC, Bessis R, Debord S, Sbaghi M and Adrian M, Phytoalexins from the Vitaceae: biosynthesis, phytoalexin gene expression in transgenic plants, antifungal activity, and metabolism. *J Agric Food Chem* **50**: 2731-2741 (2002).
2. Guerrero RF, Puertas B, Fernández MI, Palma M and Cantos-villar E, Induction of stilbenes in grapes by UV-C: Comparison of different subspecies of *Vitis*. *Innov Food Sci Emerg Technol* **11**: 231-238 (2010).
3. Beaumont P, Courtois A and Atgié C, In the shadow of resveratrol: biological activities of epsilon-viniferin. *J Physiol Biochem* **78**: 465–484 (2022).
4. Deck LM, Whalen LJ, Hunsaker LA, Royer RE and Vander Jagt DL, Activation of antioxidant Nrf2 signalling by substituted *trans* stilbenes. *Bioorg Med Chem* **25**: 1423-1430 (2017).
5. Nagumo M, Ninomiya M, Oshima N, Itoh T, Tanaka K, Nishina A and Koketsu M, Comparative analysis of stilbene and benzofuran neolignan derivatives as acetylcholinesterase inhibitors with neuroprotective and anti-inflammatory activities. *Bioorganic Med Chem Lett* **29**: 2475-2479 (2019).
6. Wu JM, Wang ZR, Hsieh TC, Bruder JL, Zou JG and Huang YZ, Mechanism of cardioprotection by resveratrol, a phenolic antioxidant presents in red wine. *Int J Mol Med* **8**: 3-17 (2001).
7. Balasubramani SP, Rahman MA and Basha SM, Synergistic action of stilbenes in Muscadine grape berry extract shows better cytotoxic potential against cancer cells than Resveratrol alone. *Biomedicines* **7**: 96 (2019).
8. Pezet R, Gindro K, Viret O and Spring JL, Glycosylation and oxidative dimerization of resveratrol are respectively associated to sensitivity and resistance of grapevine cultivars to downy mildew. *Physiol Mol Plant Pathol* **65**: 297-303 (2004).

9. Jiménez JB, Orea JM, Montero C, Ureña ÁG, Navas E, Slowing K and De Martinis D, Resveratrol treatment controls microbial flora, prolongs shelf life, and preserves nutritional quality of fruit. *J Agric Food Chem* **53**: 1526-1530 (2005).
10. Houillé B, Besseau S, Courdavault V, Oudin A, Glévarec G, Delanoue G, Guérin L, Simkin AJ, Papon N and Clastre M, Biosynthetic origin of *e*-resveratrol accumulation in grape canes during postharvest storage. *J Agric Food Chem* **63**: 1631–1638 (2015).
11. Goufo P, Singh RK and Cortez I, A reference list of phenolic compounds (including stilbenes) in grapevine (*Vitis vinifera* L.) roots, woods, canes, stems, and leaves. *Antioxidants* **9**: 398 (2020).
12. Gorena T, Sáez V, Mardones C, Vergara C, Winterhalter P and von Baer D, Influence of post-pruning storage on stilbenoid levels in *Vitis vinifera* L. canes. *Food Chem* **155**: 256–263 (2014).
13. Cebrián C, Sánchez-Gómez R, Salinas MR, Alonso GL and Zalacain A, Effect of post-pruning vine-shoots storage on the evolution of high-value compounds. *Ind Crop Prod* **109**: 730–736 (2017).
14. Zwingelstein M, Draye M, Besombes JL, Piot C and Chatel G, Viticultural wood waste as a source of polyphenols of interest: Opportunities and perspectives through conventional and emerging extraction methods. *Waste Manag* **102**: 782–794 (2019).
15. Noviello M, Caputi AF, Squeo G, Paradiso VM, Gambacorta G and Caponio F, Vine shoots as a source of *trans*-resveratrol and *ε*-viniferin: a study of 23 italian varieties. *Foods* **1**: 553 (2022).
16. Fiod Riccio BV, Fonseca-Santos B, Colerato Ferrari P and Chorilli M, Characteristics, biological properties and analytical methods of *trans*-resveratrol: A review. *Crit Rev Anal Chem* **50**: 339-358 (2020).
17. Christensen J, Nørgaard L, Bro R and Engelsen SB, Multivariate autofluorescence of intact food systems. *Chem. Rev.* **106**: 1979-1994 (2006).

18. Sikorska E, Khmelinskii I and Sikorski M, Fluorescence spectroscopy and imaging instruments for food quality evaluation, In *Evaluation technologies for food quality*, ed. by Zhong J and Wang X. Woodhead Publishing, pp. 491-533 (2019).
19. Faassen SM and Hitzmann B, Fluorescence spectroscopy and chemometric modelling for bioprocess monitoring. *Sensors* **15**: 10271-10291 (2015).
20. Cabrera-Bañegil M, Hurtado-Sánchez MC, Galeano-Díaz T and Durán-Merás I, Front-face fluorescence spectroscopy combined with second-order multivariate algorithms for the quantification of polyphenols in red wine samples. *Food Chem* **220**: 168-176 (2017).
21. Vergara C, Von Baer D, Mardones C, Wilkens A, Wernekinck K, Damm A, Macke S, Gorena T and Winterhalter P, Stilbene levels in grape cane of different cultivars in southern Chile: determination by HPLC-DAD-MS/MS method. *J Agric Food Chem* **60**: 929–933 (2012).
22. Ortiz MC, Sarabia LA, Sánchez MS and Giménez D, Identification and quantification of ciprofloxacin in urine through excitation-emission fluorescence and three-way PARAFAC calibration. *Anal Chim Acta* **642**:193-205. (2009).
23. Ortiz MC, Sarabia LA, Sánchez MS, Herrero A, Sanllorente S and Reguera C, Usefulness of PARAFAC for the quantification, identification, and description of analytical data, in *Data Handling in Science and Technology,* ed. by de la Peña AM, Goicoechea HC, Escandar GM and Olivieri AC. Elsevier Science Publisher, Amsterdam, pp. 37-81 (2015).
24. Murphy KR, Stedmon CA, Graeber D and Bro R, Fluorescence spectroscopy and multi-way techniques. PARAFAC. *Anal Methods* **5**: 6557-6566 (2013).
25. Squeo G, De Angelis D, Summo C, Pasqualone A, Caponio F and Amigo JM, Assessment of macronutrients and alpha-galactosides of texturized vegetable proteins by near infrared hyperspectral imaging. *J Food Compos Anal* **108**: 104459 (2022).

26. Lambert C, Richard T, Renouf E, Bisson J, Waffo-Téguo P, Bordenave L, Ollat N, Mérillon JM and Cluzet S, comparative analyses of stilbenoids in canes of major *Vitis vinifera* l. cultivars. *J Agric Food Chem* **61**: 11392–11399 (2013).
27. Barros A, Gironés-Vilaplana A, Teixeira A, Collado-González J, Moreno DA, Gil-Izquierdo A, Rosa E and Domínguez-Perles R, Evaluation of grape (*Vitis vinifera* L.) stems from Portuguese varieties as a resource of (poly)phenolic compounds: A comparative study. *Food Res Int* **65**: 375-384 (2014).
28. Dias C, Domínguez-Perles R, Aires A, Teixeira A, Rosa E, Barros A and Saavedra MJ, Phytochemistry and activity against digestive pathogens of grape (*Vitis vinifera* L.) stem's (poly) phenolic extracts. *LWT* **61**: 25-32 (2015).
29. Lenhardt Acković L, Zeković I, Dramićanin T, Bro R and Dramićanin MD, Modeling food fluorescence with PARAFAC, In *Reviews in Fluorescence 2017*, ed. by Gennes C. Springer Publisher, pp 161-197 (2018).
30. Poutaraud A, Latouche G, Martins S, Meyer S, Merdinoglu D and Cerovic ZG, Fast and local assessment of stilbene content in grapevine leaf by in vivo fluorometry. *J Agric Food Chem* **55**: 4913-4920 (2007).
31. Bernardes CD, Poppi RJ and Sena MM, Direct determination of *trans*-resveratrol in human plasma by spectrofluorimetry and second-order standard addition. *Talanta* **82**: 640-645 (2010).
32. Mustorgi E, Durante C, Malegori C, Greco P, Bartoletti R, Cocchi M and Casale M, An analytical approach based on excitation-emission fluorescence spectroscopy and chemometrics for the screening of prostate cancer through urine analysis: A proof–of–concept study. *Chemom Intell Lab Syst* **234**: 104752 (2023).
33. Włodarska K, Pawlak-Lemańska K, Khmelinskii I and Sikorska E, Explorative study of apple juice fluorescence in relation to antioxidant properties. *Food Chem* **210**: 593-599 (2016).

34. Squeo G, Caponio F, Paradiso VM, Summo C, Pasqualone A, Khmelinskii I and Sikorska E, Evaluation of total phenolic content in virgin olive oil using fluorescence excitation–emission spectroscopy coupled with chemometrics. *J Sci Food Agric* **99**: 2513-2520 (2019).
35. Quintanilla-Casas B, Rinnan Å, Romero A, Guardiola F, Tres A, Vichi S and Bro R, Using fluorescence excitation-emission matrices to predict bitterness and pungency of virgin olive oil: A feasibility study. *Food Chem* **395**: 133602 (2022).
36. Antônio DC, Botelho BG and Sena MM, Spectrofluorimetric determination of phenylalanine in honey by the combination of standard addition method and second-order advantage. *Food Anal Methods* **15**: 728–738 (2022).
37. Olivieri AC (ed). *Introduction to multivariate calibration: A practical approach*. Springer, Berlin (2018).
38. Westad F, Bevilacqua M and Marini F, Regression, *In Data handling in science and technology,* ed. by Marini F. Elsevier Science Publisher, Amsterdam, pp. 127-170 (2013).
39. Halberg, HFF, Bevilacqua M and Rinnan Å, Is core consistency a too conservative diagnostic? *J Chemom* e3483 (2023).

Figure Legends

Figure 1. Example of EEMs of vine shoots extracts. Contour plots of four different specimens, two from dataset A (No. 48 and 31 in Table 1; indicated as A and B) and two from dataset B (No. 68 and 67 in Table 1; indicated as C and D), having low and high TR concentration, respectively.

Figure 2. Example of UHPLC-FLD (excitation = 350 nm, emission = 380 nm) chromatogram of a vine shoots extract. The TR peak is marked.

Figure 3. Excitation and emission spectral loadings of the PARAFAC models with 1 (A), 5 (B), 6 (C), and 12 (D) components.

Figure 4. Regression line between sample mode loadings of standard solutions of TR and the relative concentration (A), and predicted *vs* measured TR concentrations in the extracts (B) for a 6-components PARAFAC model (component 1 sample mode scores were used for the regression).

Figure 5. Regression line between sample mode loadings of standard solutions of TR and the relative concentration (A), and predicted *vs* measured TR concentrations in the extracts (B) for a 12-components PARAFAC model (component 2 sample mode scores were used for the regression).

Appendices

Submitted as Supplementary material.

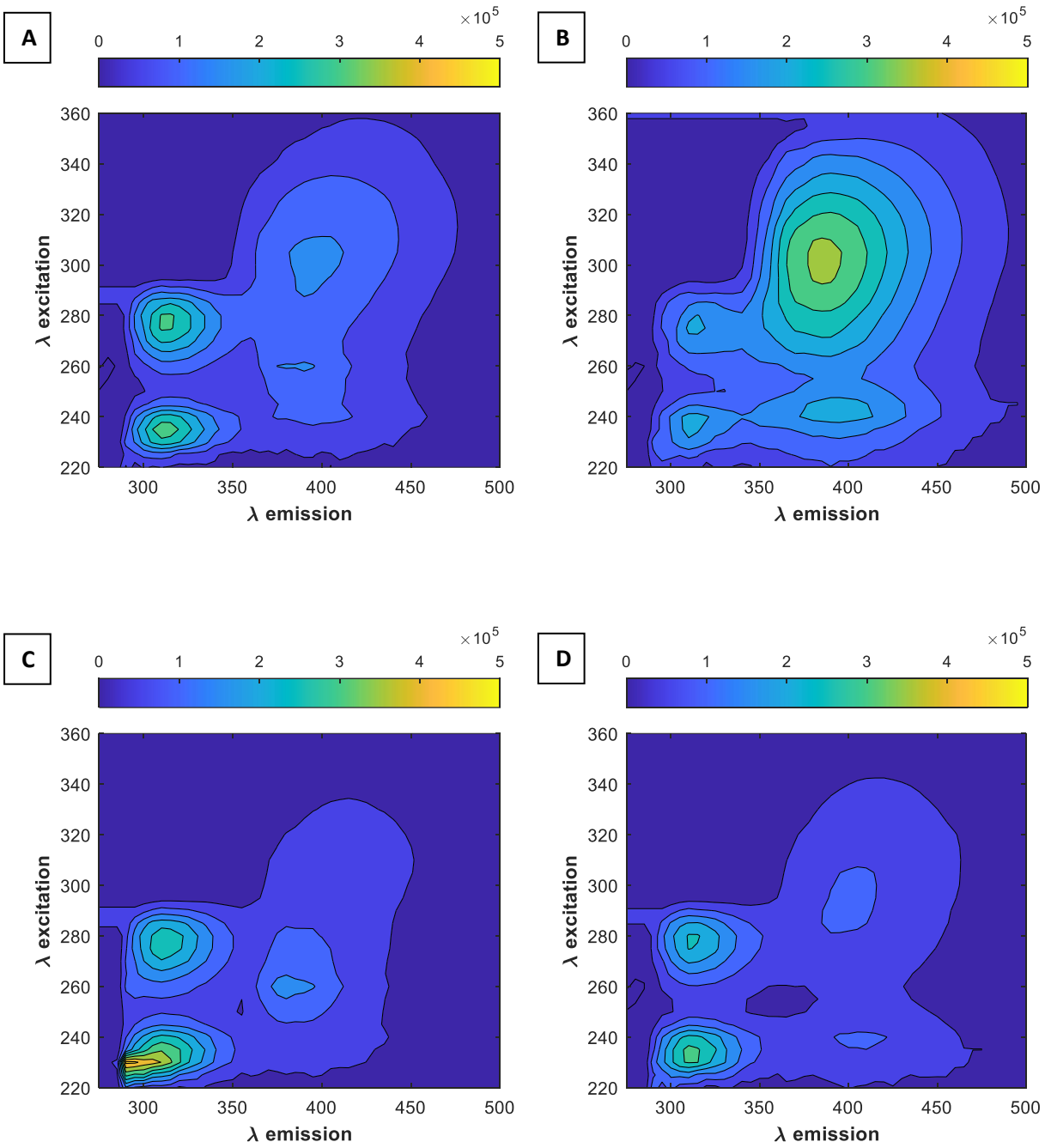
A
B
C
D
×10^5
0 1 2 3 4 5
360 340 320 300 280 260 240 220
λ excitation
300 350 400 450 500
λ emission

Figure 1.

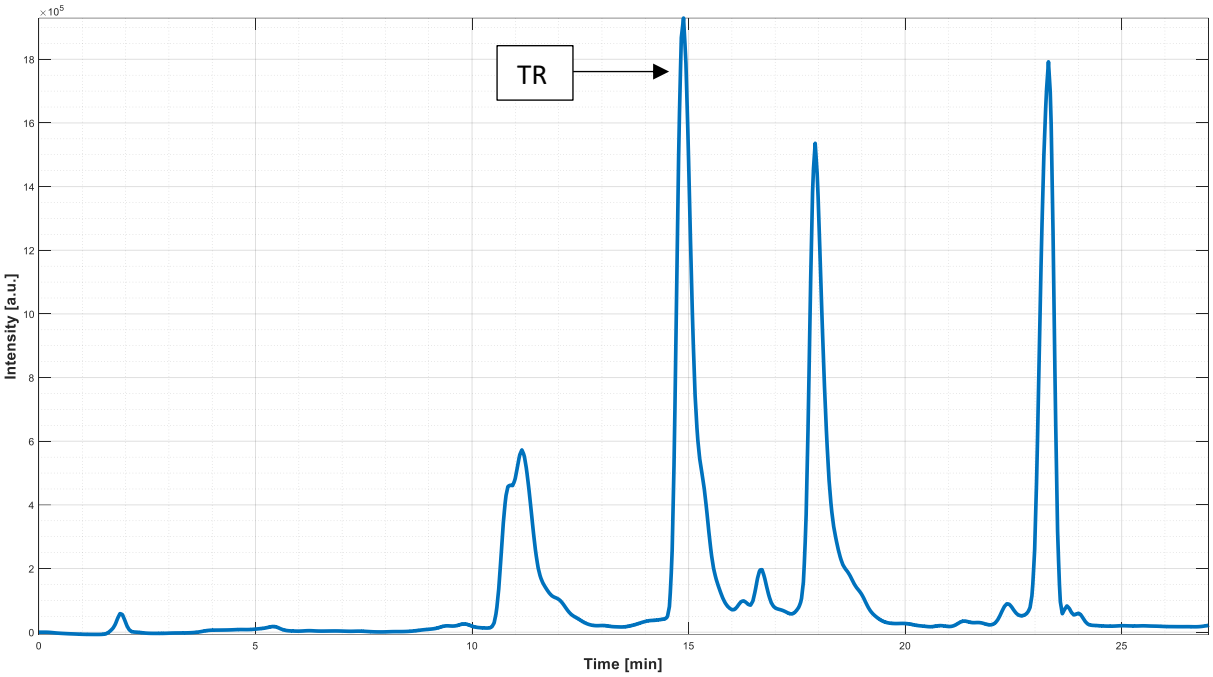

Figure 2.

A

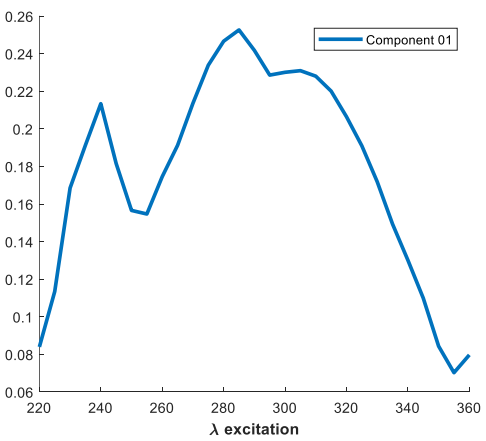
Component 01
λ excitation

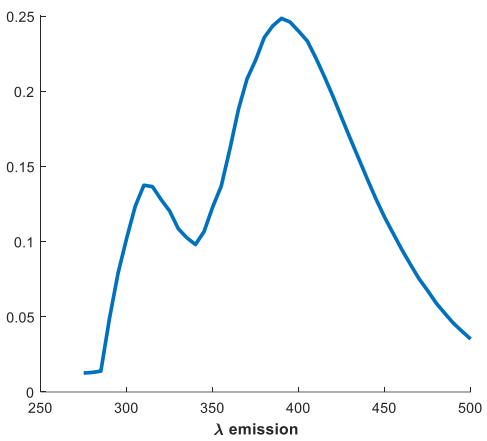
λ emission

B

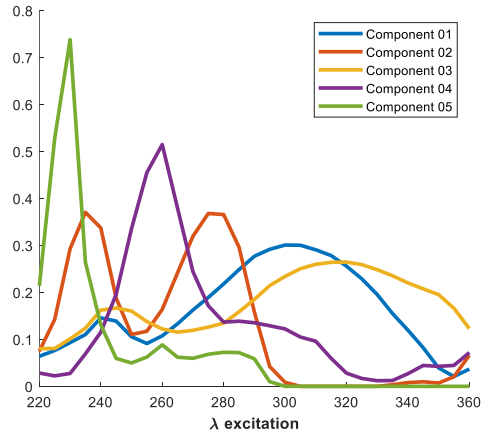
Component 01
Component 02
Component 03
Component 04
Component 05
λ excitation

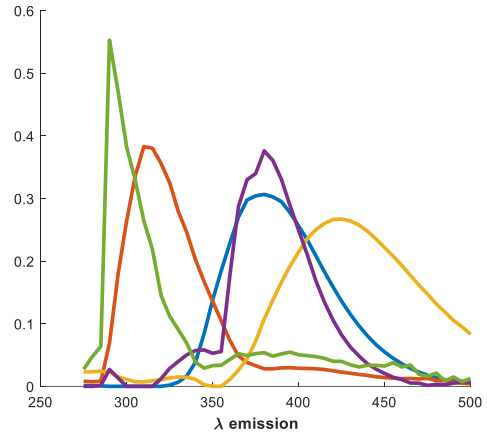
λ emission

C

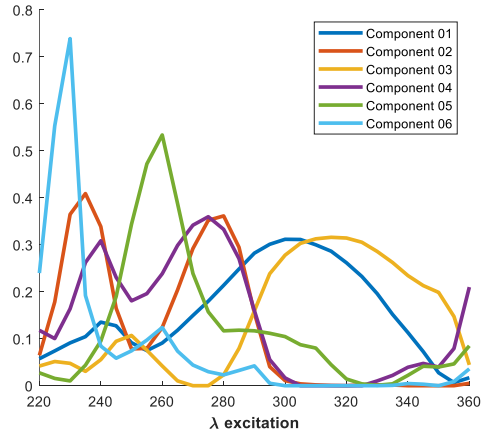
Component 01
Component 02
Component 03
Component 04
Component 05
Component 06
λ excitation

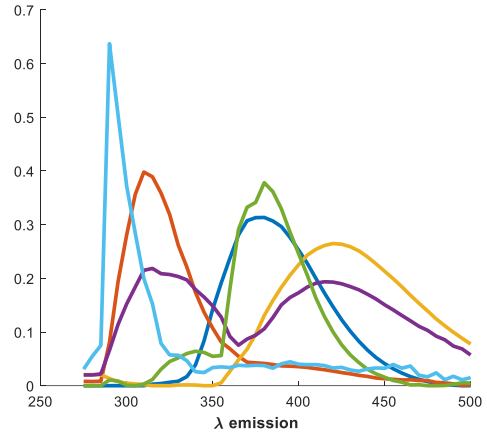
λ emission

D

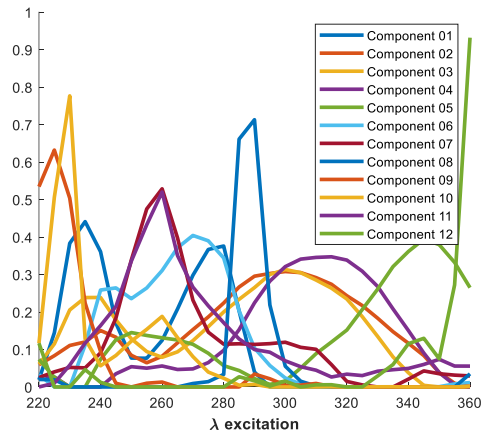
Component 01
Component 02
Component 03
Component 04
Component 05
Component 06
Component 07
Component 08
Component 09
Component 10
Component 11
Component 12
λ excitation

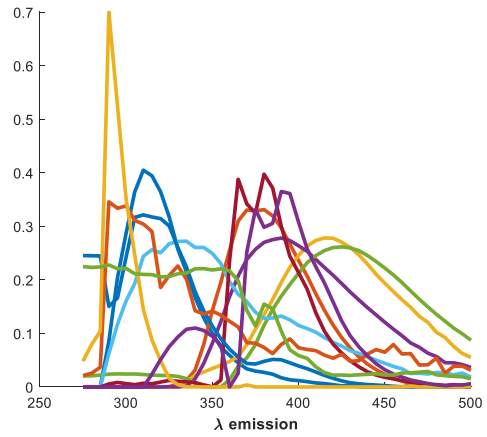
λ emission

Figure 3.

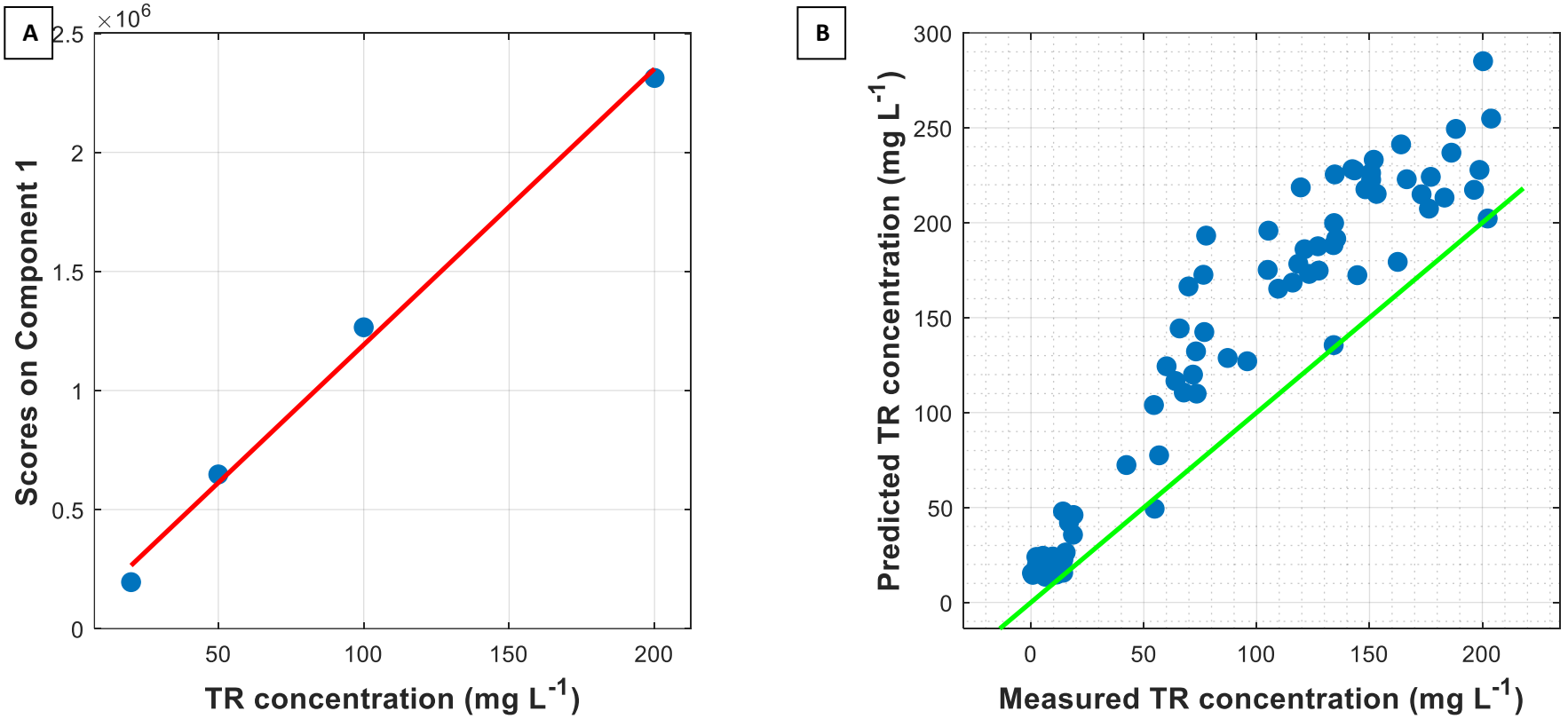
A
×10^6
2.5
2
1.5
1
0.5
0
Scores on Component 1
50
100
150
200
TR concentration (mg L^-1)
B
300
250
200
150
100
50
0
Predicted TR concentration (mg L^-1)
0
50
100
150
200
Measured TR concentration (mg L^-1)

Figure 4.

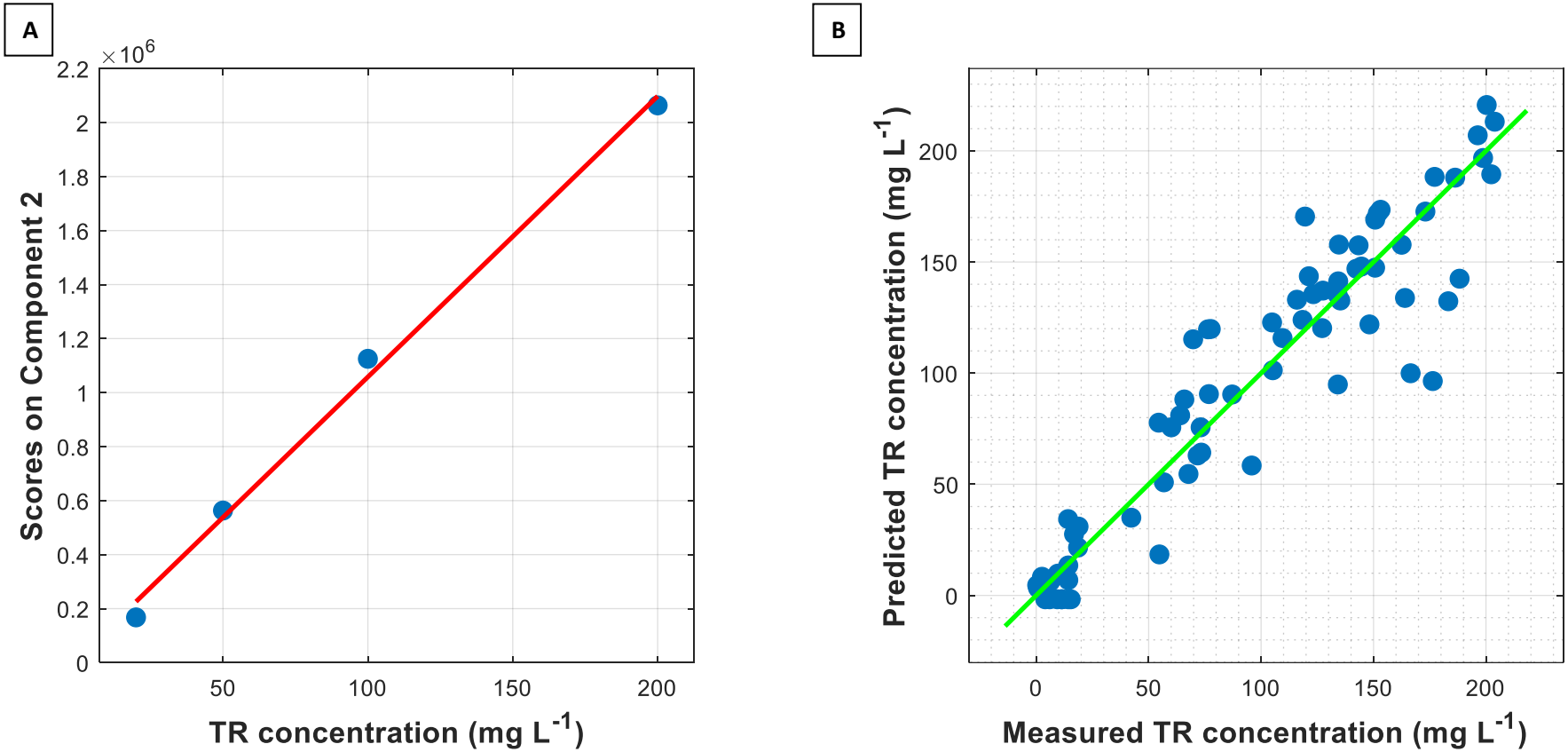
A
×10^6
2.2
2
1.8
1.6
1.4
1.2
1
0.8
0.6
0.4
0.2
0
Scores on Component 2
50
100
150
200
TR concentration (mg L^-1)
B
Predicted TR concentration (mg L^-1)
200
150
100
50
0
0
50
100
150
200
Measured TR concentration (mg L^-1)

Figure 5.

Table 1. T*rans*-resveratrol concentration (mg L^{-1}) in the vine shoots extracts.

Set	#	Variety	TR concentration †
A	1	Aglianico	76.79 ± 0.75
A	2	Bianco d'Alessano	115.93 ± 0.65
A	3	Bianco d'Alessano	127.47 ± 0.60
A	4	Bombino Bianco	123.22 ± 0.55
A	5	Bombino Bianco	134.13 ± 0.23
A	6	Bombino Nero	105.20 ± 0.47
A	7	Bombino Nero	121.22 ± 1.96
A	8	Ciliegiolo	95.81 ± 0.15
A	9	Ciliegiolo	104.88 ± 0.46
A	10	Fiano Bianco d'Avellino	143.34 ± 0.08
A	11	Fiano Bianco d'Avellino	151.88 ± 0.20
A	12	Italia	150.73 ± 0.26
A	13	Italia	153.15 ± 0.98
A	14	Malvasia Bianca	69.78 ± 0.12
A	15	Malvasia Bianca	76.41 ± 0.08
A	16	Malvasia Nera di Brindisi	73.11 ± 0.72
A	17	Malvasia Nera di Brindisi	73.39 ± 0.74
A	18	Maresco Bianco	109.54 ± 0.34
A	19	Maresco Bianco	118.45 ± 1.96
A	20	Minutolo Bianco	134.03 ± 0.80
A	21	Minutolo Bianco	134.30 ± 0.61
A	22	Montepulciano	183.23 ± 0.39
A	23	Montepulciano	188.27 ± 1.44
A	24	Negroamaro	144.60 ± 0.84
A	25	Negroamaro	162.49 ± 0.80
A	26	Negroamaro	173.06 ± 0.01
A	27	Negroamaro	177.16 ± 0.57
A	28	Negroamaro	198.73 ± 0.59
A	29	Negroamaro	200.33 ± 0.31
A	30	Negroamaro	202.35 ± 0.46
A	31	Negroamaro	203.90 ± 0.29
A	32	Nero di Troia	186.30 ± 0.01
A	33	Nero di Troia	196.33 ± 0.25
A	34	Notardomenico	163.98 ± 0.41
A	35	Ottavianello	67.71 ± 0.14
A	36	Ottavianello	71.78 ± 0.57
A	37	Palieri	166.49 ± 0.05
A	38	Palieri	176.34 ± 0.92
A	39	Primitivo	60.08 ± 0.19
A	40	Primitivo	65.86 ± 0.74
A	41	Primitivo	127.14 ± 0.88
A	42	Primitivo	148.18 ± 0.92
A	43	Primitivo	150.70 ± 0.35
A	44	Sangiovese	77.61 ± 0.31
A	45	Sangiovese	87.14 ± 0.07

A	46	Susumaniello	135.24 ± 0.45
A	47	Susumaniello	142.38 ± 0.10
A	48	Trebbiano	42.29 ± 0.56
A	49	Verdeca	54.31 ± 0.22
A	50	Verdeca	64.00 ± 0.08
A	51	Vittoria	119.54 ± 0.04
A	52	Vittoria	134.59 ± 0.51
B	53	Aleatico	2.38 ± 0.09
B	54	Aleatico	5.33 ± 0.27
B	55	Alicante	14.26 ± 0.25
B	56	Alicante	15.35 ± 0.02
B	57	Ciliegiolo	4.11 ± 0.06
B	58	Ciliegiolo	6.28 ± 0.05
B	59	Italia	14.18 ± 0.12
B	60	Italia	16.81 ± 0.04
B	61	Lambrusco	14.26 ± 0.06
B	62	Lambrusco	15.30 ± 0.19
B	63	Malvasia Bianca	0.42 ± 0.01
B	64	Moscato	11.31 ± 0.05
B	65	Moscato	11.34 ± 0.02
B	66	Palieri	54.78 ± 0.01
B	67	Palieri	56.76 ± 0.05
B	68	Primitivo	0.79 ± 0.02
B	69	Primitivo	2.58 ± 0.08
B	70	Sangiovese	9.37 ± 0.01
B	71	Sangiovese	9.62 ± 0.03
B	72	Susumaniello	4.01 ± 0.03
B	73	Susumaniello	5.97 ± 0.24
B	74	Vittoria	18.60 ± 0.05
B	75	Vittoria	18.83 ± 0.01

† Mean ± standard deviation of two technical replicates.

Table 2. Results of PARAFAC decomposition on the augmented three-way array (79 × 29 × 46).

Number of components	Core consistency (%)	Split-half quality (%) †	Explained variance (%)	Correlation excitation ‡	Correlation emission ‡	Best correlated component
1	100	99.77	81.14	0.874	0.857	Component 1
2	99.88	99.66	96.74	0.873	0.909	Component 1
3	95.68	81.17	97.84	0.900	0.994	Component 1
4	92.77	69.30	98.41	0.906	0.996	Component 1
5	83.26	77.80	99.11	0.972	0.998	Component 1
6	< 0	16.52	99.29	0.976	0.995	Component 1
7	< 0	36.07	99.49	0.929	0.995	Component 2
8	< 0	36.63	99.62	0.933	0.995	Component 1
9	< 0	0	99.60	0.818	0.990	Component 4
10	< 0	0	99.72	0.959	0.997	Component 1
11	< 0	0	99.75	0.940	0.997	Component 1
12	< 0	0	99.80	0.989	0.985	Component 2

† Mean value of 10 random splits.

‡ Pearson's linear correlation coefficient between the loadings of the excitation/emission mode of the selected PARAFAC component and the reference excitation/emission spectra of TR standard solution.

Table 3. Results of the PARAFAC based calibration.

	Calibration		**Prediction**			
Number of components	R^2	RMSEC (mg L^{-1})	R^2	RMSEP (mg L^{-1})	RE (%)	RPD
5	0.996	4.52	-0.182	70.85	76	0.93
6	0.995	4.91	0.346	52.69	57	1.26
12	0.995	4.75	0.880	22.57	24	2.91

RMSE, root mean square error; RE, percentage relative error; RPD, relative prediction deviation.

Table 4. Results of the NPLS regression models.

	Calibration					Cross-validation		Prediction		
Range	LV	X e.v.	Y e.v.	R^2	RMSEC	R^2	RMSECV	R^2	RMSEP	RE	RPD
Full emission range	8	98.46	97.54	0.975	10.34	0.947	16.02	0.914	19.47	20	3.33
Reduced emission range	8	99.18	97.11	0.971	11.21	0.943	16.27	0.915	20.25	21	3.20

LV, number of latent variables; e.v., percentage of explained variance of X and Y; RMSE, root mean square error in mg L^{-1}; RE, percentage relative error; RPD, relative prediction deviation.

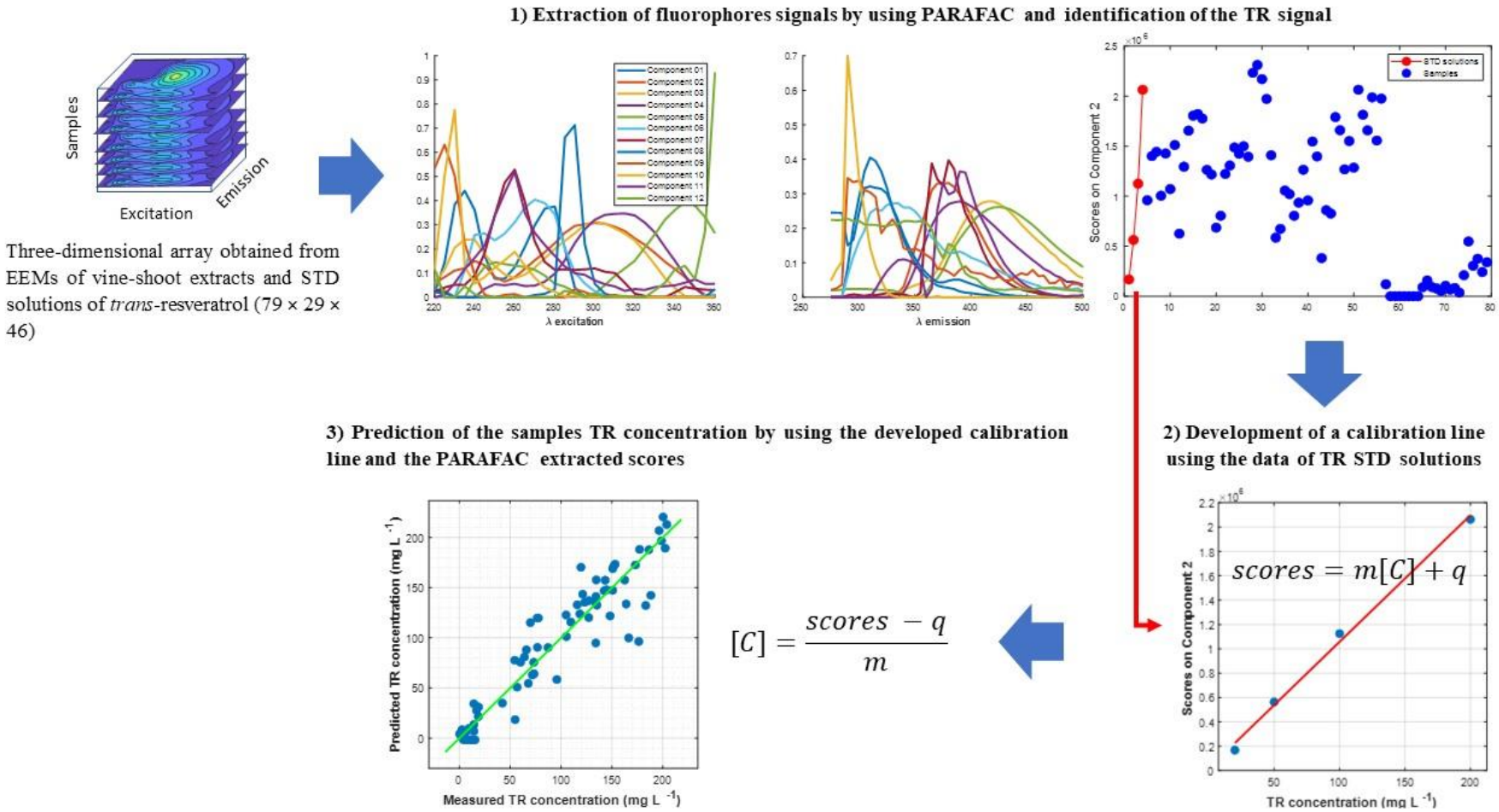

Figure S1. PARAFAC based calibration scheme.

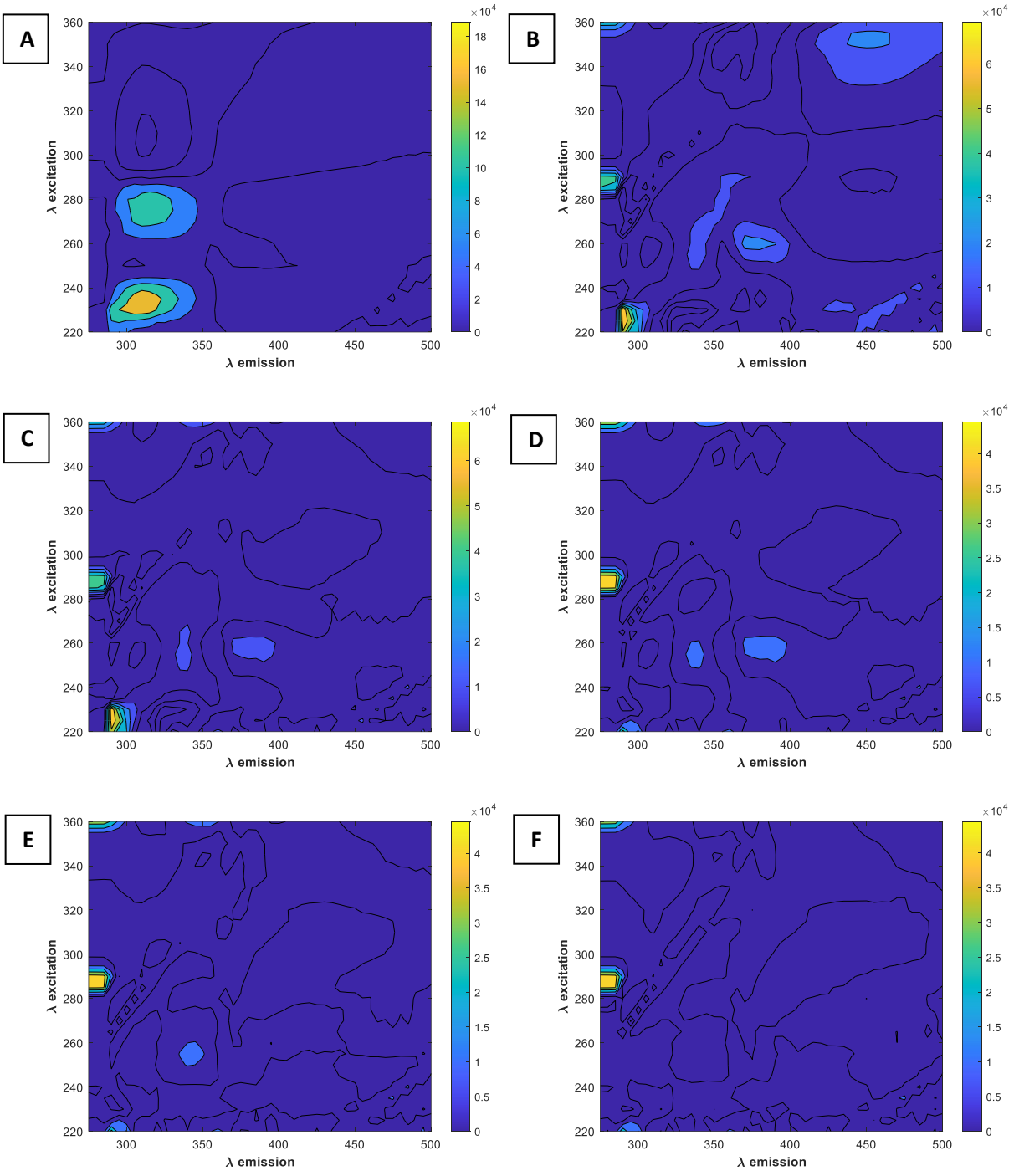
A
B
C
D
E
F
λ excitation
λ emission
220
240
260
280
300
320
340
360
300
350
400
450
500
×10^4

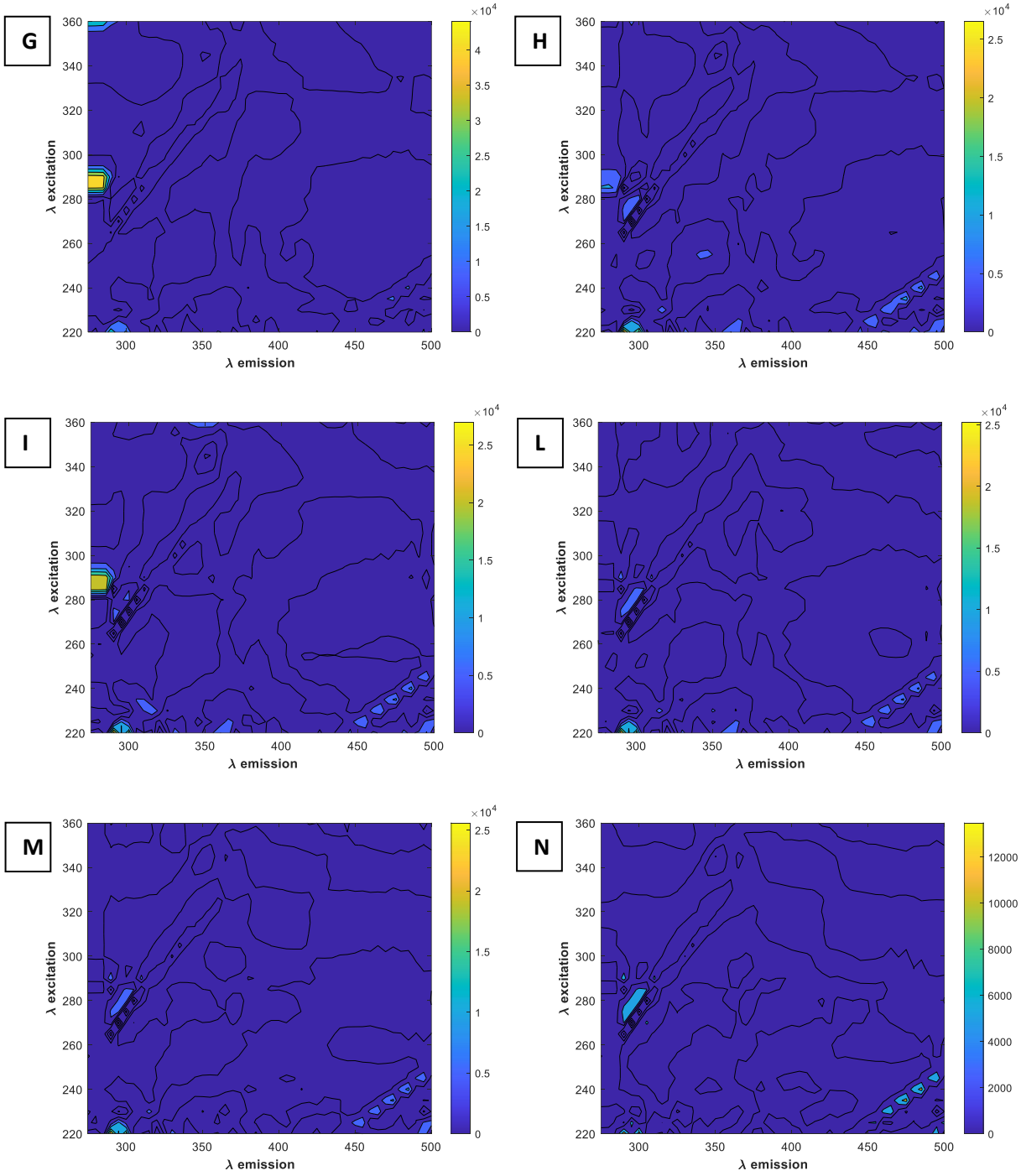

Figure S2. Average PARAFAC residuals for an increasing number of components from 1 (A) to 12 (N).

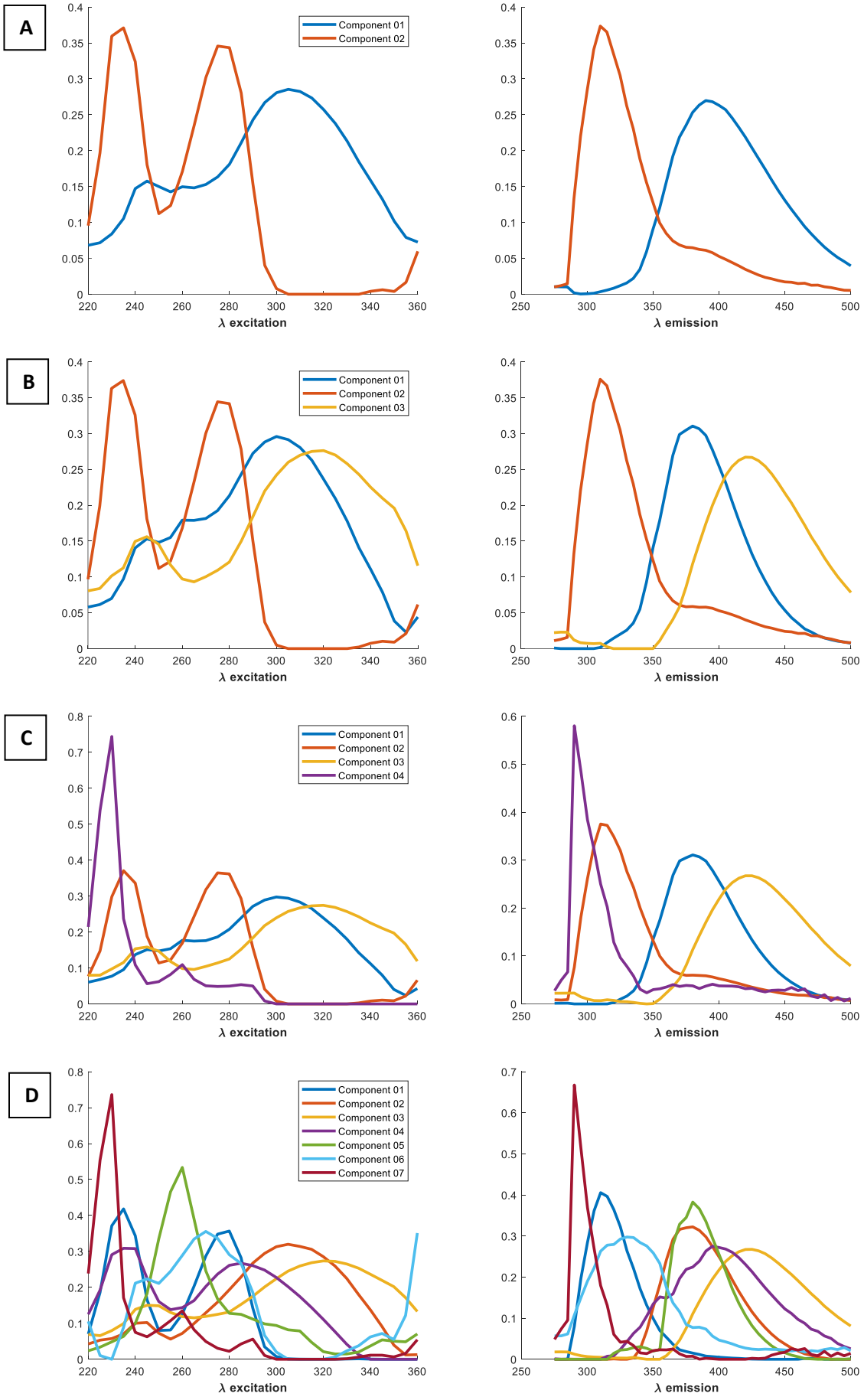
A
Component 01
Component 02
λ excitation
λ emission
B
Component 01
Component 02
Component 03
λ excitation
λ emission
C
Component 01
Component 02
Component 03
Component 04
λ excitation
λ emission
D
Component 01
Component 02
Component 03
Component 04
Component 05
Component 06
Component 07
λ excitation
λ emission

E

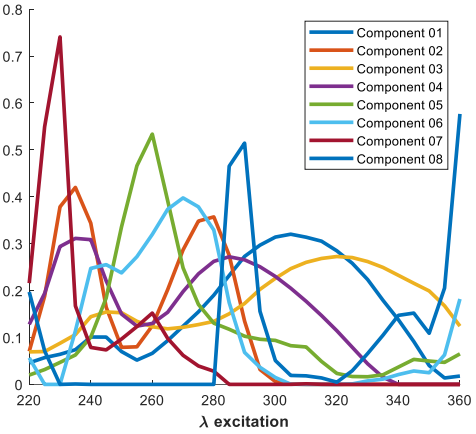
Component 01
Component 02
Component 03
Component 04
Component 05
Component 06
Component 07
Component 08
λ excitation

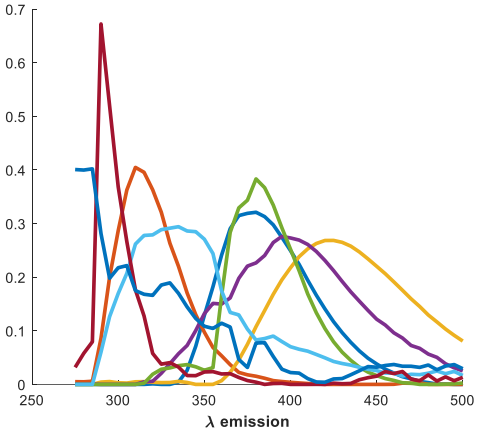
λ emission

F

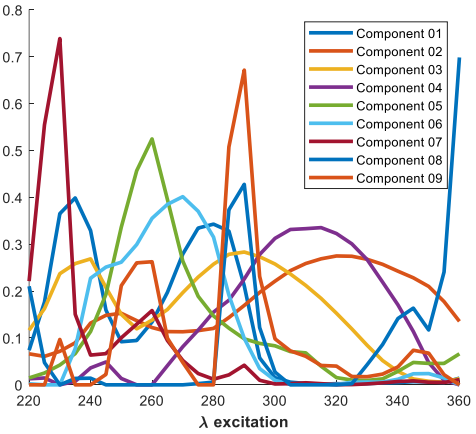
Component 01
Component 02
Component 03
Component 04
Component 05
Component 06
Component 07
Component 08
Component 09
λ excitation

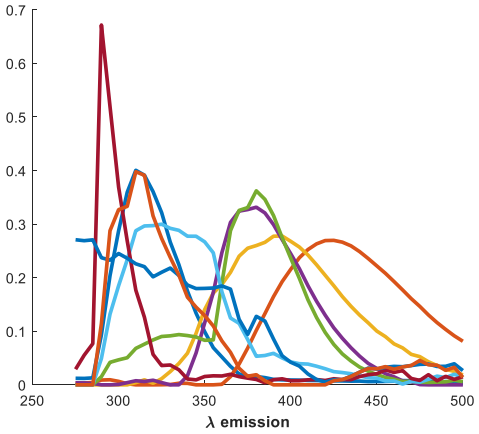
λ emission

G

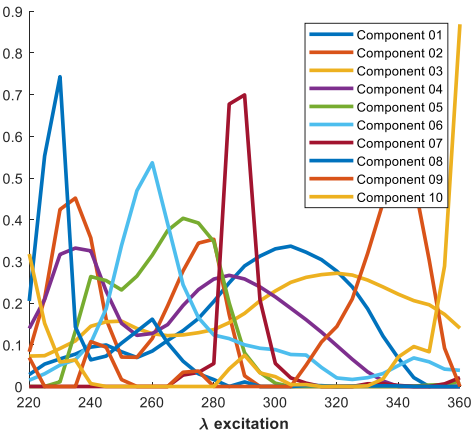
Component 01
Component 02
Component 03
Component 04
Component 05
Component 06
Component 07
Component 08
Component 09
Component 10
λ excitation

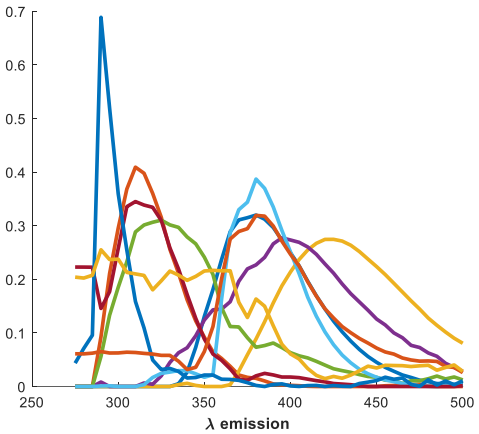
λ emission

H

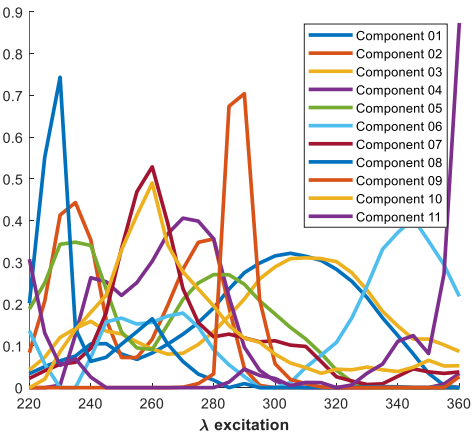
Component 01
Component 02
Component 03
Component 04
Component 05
Component 06
Component 07
Component 08
Component 09
Component 10
Component 11
λ excitation

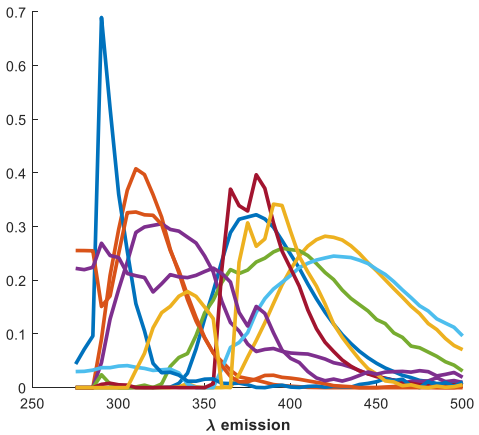
λ emission

Figure S3. Excitation and emission spectral loadings of the PARAFAC models with an increasing number of components from 2 to 4 (A-C) and from 7 to 11 (D-H).

Table S1. Descriptive statistics of the calibration and validation sets used for NPLS regression.

Set	Number of samples	Min (mg L^{-1})	Max (mg L^{-1})	Mean (mg L^{-1})	SD (mg L^{-1})
Calibration	50	0.42	203.90	91.19	66.57
Validation	25	2.58	198.73	96.68	64.84

Table S2. Predicted TR concentration (mg L^{-1}) in vine shoots ethanolic extracts by the best PARAFAC and NPLS models calculated. †

Set	#	Variety	TR concentration	PARAFAC based regression predictions	NPLS predictions
A	1	Aglianico	76.79	90.57	
A	2	Bianco d'Alessano	115.93	133.04	
A	3	Bianco d'Alessano	127.47	137.12	121.19
A	4	Bombino Bianco	123.22	135.52	
A	5	Bombino Bianco	134.13	94.90	
A	6	Bombino Nero	105.20	101.30	
A	7	Bombino Nero	121.22	143.59	
A	8	Ciliegiolo	95.81	58.45	142.34
A	9	Ciliegiolo	104.88	122.81	
A	10	Fiano Bianco d'Avellino	143.34	157.49	152.19
A	11	Fiano Bianco d'Avellino	151.88	171.88	
A	12	Italia	150.73	169.06	
A	13	Italia	153.15	173.49	
A	14	Malvasia Bianca	69.78	115.23	
A	15	Malvasia Bianca	76.41	119.73	85.65
A	16	Malvasia Nera di Brindisi	73.11	75.63	
A	17	Malvasia Nera di Brindisi	73.39	64.25	71.21
A	18	Maresco Bianco	109.54	115.80	94.55
A	19	Maresco Bianco	118.45	123.94	
A	20	Minutolo Bianco	134.03	135.28	
A	21	Minutolo Bianco	134.30	141.30	127.30
A	22	Montepulciano	183.23	132.34	
A	23	Montepulciano	188.27	142.50	
A	24	Negroamaro	144.60	147.96	
A	25	Negroamaro	162.49	157.76	
A	26	Negroamaro	173.06	172.69	
A	27	Negroamaro	177.16	188.30	
A	28	Negroamaro	198.73	196.80	189.62
A	29	Negroamaro	200.33	220.62	
A	30	Negroamaro	202.35	189.45	
A	31	Negroamaro	203.90	213.11	
A	32	Nero di Troia	186.30	187.94	166.24
A	33	Nero di Troia	196.33	206.99	190.08
A	34	Notardomenico	163.98	133.83	
A	35	Ottavianello	67.71	54.64	
A	36	Ottavianello	71.78	62.98	
A	37	Palieri	166.49	99.94	
A	38	Palieri	176.34	96.43	150.43

A	39	Primitivo	60.08	75.62	
A	40	Primitivo	65.86	88.17	
A	41	Primitivo	127.14	120.25	175.37
A	42	Primitivo	148.18	121.92	
A	43	Primitivo	150.70	147.44	180.96
A	44	Sangiovese	77.61	119.86	
A	45	Sangiovese	87.14	90.40	82.18
A	46	Susumaniello	135.24	132.68	
A	47	Susumaniello	142.38	146.96	143.89
A	48	Trebbiano	42.29	34.97	
A	49	Verdeca	54.31	77.72	
A	50	Verdeca	64.00	81.02	
A	51	Vittoria	119.54	170.44	145.57
A	52	Vittoria	134.59	157.84	152.50
B	53	Aleatico	2.38	7.13	
B	54	Aleatico	5.33	5.87	
B	55	Alicante	14.26	-1.73	
B	56	Alicante	15.35	-1.73	-4.01
B	57	Ciliegiolo	4.11	1.80	
B	58	Ciliegiolo	6.28	6.28	
B	59	Italia	14.18	34.34	23.81
B	60	Italia	16.81	27.56	
B	61	Lambrusco	14.26	6.91	4.91
B	62	Lambrusco	15.30	13.49	
B	63	Malvasia Bianca	0.42	4.61	
B	64	Moscato	11.31	-1.73	
B	65	Moscato	11.34	-1.73	
B	66	Palieri	54.78	18.45	
B	67	Palieri	56.76	50.88	35.78
B	68	Primitivo	0.79	3.32	
B	69	Primitivo	2.58	8.39	9.42
B	70	Sangiovese	9.37	-1.73	
B	71	Sangiovese	9.62	9.81	19.53
B	72	Susumaniello	4.01	-1.73	
B	73	Susumaniello	5.97	-1.73	20.37
B	74	Vittoria	18.60	21.56	
B	75	Vittoria	18.83	30.97	23.12

† The best PARAFAC based model was a 12-components model calculated by using the whole emission range. The best NPLS model was the one calculated by using the whole emission range.